# LDA simulations of pressure-induced anomalies in $c/a$ and electric-field gradients for Zn and Cd

D. L. Novikov* and A. J. Freeman
*Science and Technology Center for Superconductivity, Department of Physics and Astronomy, Northwestern University, Evanston, Illinois 60208*

N. E. Christensen and A. Svane
*Institute of Physics and Astronomy, Aarhus University, DK-8000 Aarhus C, Denmark*

C. O. Rodriguez
*Instituto de Fisica de Liquidos y Sistemas Biológicos, Grupo Fisica del Sólido, Casilla de Correo 565, La Plata 1900, Argentina*
(Received 7 March 1997)

We present results of *ab initio* simulations of the effect of hydrostatic pressure on the electronic structure, lattice parameters, and electric-field gradients (EFG) for hcp Zn and Cd using the full-potential linear muffin-tin orbital method in conjunction with the new Perdew-Burke-Ernzerhof generalized gradient approximation (GGA) to the density functional for exchange correlation. Theoretical equilibrium volumes for Zn and Cd are found to be in excellent agreement with experiment (whereas non-GGA corrected local density approximation underestimates them by as much as 10%). We find an anomaly in the pressure dependence of $c/a$ at reduced unit cell volumes (at $V/V_0 \simeq 0.89$ for Zn and in a broad region from $V/V_0 = 0.92$ to 0.85 for Cd) and a similar anomaly in the EFG tensor. At the same time we do not find the electronic topological transition due to the destruction of a giant Kohn anomaly which was previously thought to be responsible for the lattice anomalies in Zn. [S0163-1829(97)02035-3]

## I. INTRODUCTION

Understanding the structural and electronic properties of hexagonal-close-packed (hcp) Zn and Cd is of fundamental importance. The fact that these metals have unusually large $c/a$ ratios (1.856 for Zn and 1.886 for Cd) in comparison to the ideal value of $\sqrt{8/3} \approx 1.633$ makes them unique in the family of hcp metals. Large $c/a$ ratios make many of their solid-state properties highly anisotropic and so have been extensively studied both experimentally[1–6] and theoretically.[7–11]. Although the electronic and lattice properties of Zn and Cd have been studied for many years, recent publications on Zn by Takemura[12] on high-pressure powder x-ray diffraction experiments (at room temperature) and Potzel *et al.*[13,14] on $^{67}$Zn Mössbauer studies (at 4.2 K) have renewed interest in these metals, and seem to resolve the question on the anomalous lattice properties of Zn under hydrostatic pressure. The earlier studies by Lynch and Drickamer[15] which found a nonmonotonic pressure dependence of the $c/a$ ratio in Zn and Cd are contradicted by more recent results by Schlute *et al.*[16] where $c/a$ did not show such a behavior. Takemura has shown[12] that the volume dependence of $c/a$ in Zn changes its slope at $V/V_0 = 0.893$ ($P = 9.1$ GPa), while Potzel *et al.*[13] found a drastic drop (by a factor of 2) of the Lamb-Mössbauer factor indicating a drastic softening of low-frequency acoustic and optical phonons at $V/V_0 \approx 0.915$ ($P = 6.6$ GPa). A change in the curvature of the electric-field gradient (EFG) dependence on pressure was also observed.[13,14]

From theoretical studies, it is quite clear that the electronic structure of Zn plays a critical role in these phenomena. As shown by Bodenstedt *et al.*,[17] the large $c/a$ ratio in Zn and the consequent anisotropic lattice properties are caused by the asymmetric charge distribution of the $p$ electrons. As a result, the Fermi surface of Zn (and its isoelectronic counterpart Cd) differs from that of normal hcp metals—a difference that gives rise to the so-called giant Kohn anomaly. When the Fermi level lies in the energy gap corresponding to a certain reciprocal-lattice vector $\mathbf{G}$, so that $2k_F = |\mathbf{G}|$ is satisfied, a giant Kohn anomaly appears at $\mathbf{q} \approx 0$, i.e., in the long-wavelength region. This anomaly can substantially affect low-energy acoustic phonons, i.e., produce abrupt changes of phonon frequencies at wave vectors which are related to extremal dimensions of the Fermi surface.[18] The giant Kohn anomaly in Cd was observed in an inelastic neutron scattering experiment by Chernyshov *et al.*[19] Recent linearized augmented plane-wave calculations,[13,14] performed at several experimental lattice parameters without complete structure optimization, suggest that a collapse of the giant Kohn anomaly induced by pressure is responsible for phonon softening at $V/V_0 \approx 0.915$ and possibly also of the anomalous behavior of the $c/a$ ratio. Unfortunately, no complete theoretical analysis of the lattice behavior of Zn under pressure exists so far. An earlier linear muffin-tin orbital method (LMTO) calculation[10] of the volume dependence of the axial ratio for Zn seems to reproduce the anomaly around $V/V_0 = 0.92$, but this could be questionable because of (i) the use of the atomic-sphere approximation (ASA) and (ii) the use of adjusted correction terms so as to reproduce the experimental value at atmospheric pressure.

The main reason behind the lack of lattice parameter determinations from ''first principles'' was most probably[11] the failure of the local density approximation (LDA) to reproduce the correct equilibrium volume of hcp Zn and Cd at zero pressure. The error in the equilibrium volume can be as large as 10% in $V/V_0$, depending on the type of exchange-

 

correlation potential used.[11] This was also found by earlier[20,21] calculations, and these further reproduced an anomaly in $c/a$ *near* 1.73, but not exactly at $\sqrt{3}$. The analysis of the calculations could not relate the anomaly to a topological effect in the band structure at a specific point in the Brillouin zone. This is in agreement with the results of the present work presented and discussed below.

Clearly, *ab initio* full-potential simulations of the lattice behavior in Zn and Cd with pressure are needed. In this paper, we report results of the LDA based full-potential LMTO simulation of the lattice and electronic properties for hcp Zn and Cd. In Sec. II we present results of different approaches to overcome the LDA induced errors in equilibrium volume determinations. We show that exploiting the new Perdew-Burke-Ernzerhof generalized gradient approximation[22] (PBE-GGA) corrects the problem. In Sec. III we discuss results of *ab initio* simulations of the effects of hydrostatic pressure on the lattice parameters, unit cell volume, bulk moduli, volume and uniaxial compressibilities, and electric-field gradient (EFG) tensor and electronic structure for hcp Zn and Cd. We show that at reduced volume, the anomaly in the $c/a$ ratio does exist and occurs at $V/V_0=0.89$ for Zn and over a range, $V/V_0=0.92$ to 0.85 for Cd. We also find that the volume dependence of the EFG tensor for Zn and Cd is very similar to the one for the axial ratio and also exhibits the anomalies at the same ''critical'' volumes. Moreover, we find a certain $V/V_0$ interval where the total-energy curve versus $c/a$ shows a double-well structure with an extremely small energy barrier that yields an uncertainty in the determination of the equilibrium lattice parameter, which we connect with the possibility of a sort of disorder in the system. On the other hand, our results do not confirm the idea[13,14] that the electronic topological transition (ETT) caused by the destruction of a giant Kohn anomaly is the driving force for the lattice and phonon anomalies observed in Ref. 12.

## II. CHOICE OF COMPUTATIONAL TECHNIQUE

As we mentioned in the Introduction, the conventional LDA approach fails to reproduce correctly the equilibrium volume for hcp Zn and Cd. This is very unfortunate, if one wants to study the lattice properties of these metals, especially under hydrostatic pressure. In order to find out how to improve the LDA results we have examined different corrections to the LDA and we have applied different band structure methods. The latter are various implementations of the linear methods.[23,24] Accurate predictions of structural parameters cannot be made if shape approximations are made as in the ASA that employs spherically symmetrized potentials. Full-potential (FP) implementations, such as the full-potential linear augmented plane-wave (FLAPW) (Ref. 25) or the FP-LMTO (Ref. 26) schemes are needed.

In order to compare different energy functionals and methods of calculation, we examine the zero-temperature isotherm (pressure-volume, $P$-$V$ relation) for Zn. First, we used conventional LDA and applied the FP-LMTO method.[26] The calculated $P$-$V$ relation differs substantially from experiment[12,27] as can be seen from Fig. 1. The equilibrium volume is 10–11 % too small indicating a substantial overbinding. We first examined whether this error could be

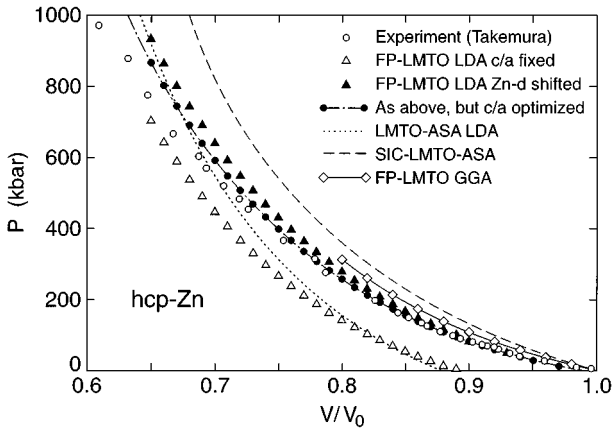


FIG. 1. The zero-temperature pressure-volume relation for Zn calculated by using various energy functionals and different band-structure methods as described in the text. Experimental points (open circles) are from Takemura (Ref. 12).

caused by numerical inaccuracies in the band-structure calculations or from application of a too small basis set. An independent LMTO-ASA calculation (dotted curve in Fig. 1) gives essentially the same equilibrium volume as the FP-LMTO volume (open triangles), but the pressure rises more rapidly with lattice compression. This difference is due to the use of ASA. Another FP-LMTO calculation using a completely different computer code[28] gave results that agree with those represented by the open triangles when a similar basis set was applied.

One might suspect that an extension of the basis set could affect the calculated energies. Especially in a case like the present one where the 3$d$ states must be included as band states, a simultaneous inclusion of 4$d$ in the basis (in the same energy panel) could be important. By expanding the basis we only found a small change in the equilibrium volume (less than 0.5%). Consequently, the error was ascribed to the LDA, and several ways of correcting for this were examined. The dashed curve in Fig. 1 represents the self-interaction corrected LMTO-ASA (SIC-LMTO-ASA) (Refs. 29,30) results. The theoretical equilibrium volume is now in perfect agreement with experiment. The fact that the $P$-$V$ relation is too steep is due to the ASA; the dashed and the dotted curves in Fig. 1 are parallel. The calculations given by the diamonds and labeled FP-LMTO-GGA include generalized gradient corrections.[31] Also the GGA yield an equilibrium volume that agrees with experiment.

In order to understand the impact of GGA on the electronic band structure we compared the energy bands of Zn along several high-symmetry directions in the BZ calculated with and without the GGA corrections and found them to be practically identical. Therefore the GGA corrections to the $P$-$V$ relation in this case are exclusively due to changes in the Coulomb interactions in the total-energy functional. The correction mechanism is then different from that of the SIC or from that represented by the filled triangles in Fig. 1, which is a standard LDA calculation except for the fact that the Zn-3$d$ states were shifted down by 2 eV in all iterations towards self-consistency. This reduces the hybridization between the 3$d$ states and the remaining valence states, and thus the overbinding is reduced. The resulting equilibribrium

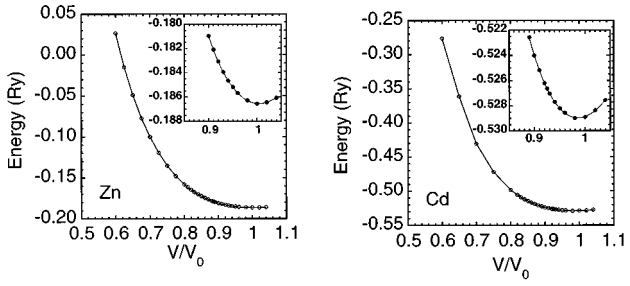


FIG. 2. FP-LMTO total energy as a function of volume for hcp Zn and Cd with $c/a$ optimized for each volume (point shown). The insets show the total-energy curves around their minima.

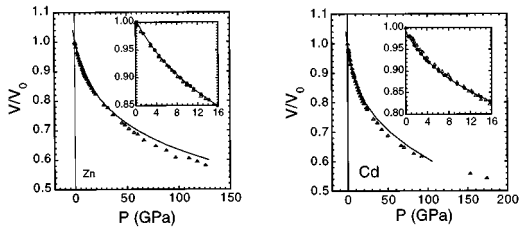


FIG. 3. The calculated pressure-volume relationship (solid lines) and experimental data (open triangles) by Takemura for hcp Zn and Cd (Refs. 12, 27, and 40). The insets show the data in the low pressure region where the calculated data is shown as solid circles.

volume is only 1% smaller than observed.

The calculations in Fig. 1 described so far were all performed for a fixed $c/a$ ratio. Now, consider the black dots connected by the full-line curve in Fig. 1 which are the results obtained when the above-mentioned downshift is applied *and* the $c/a$ ratio is optimized at each volume simultaneously via total-energy calculations. Among those discussed here, the results of this calculation agree best with experiments in the pressure range 0–400 kbar. At higher pressures, the experiments gradually approach the standard LDA results. This means that the downshift of the 3*d* states should be reduced as the compression widens the bands. This is not surprising. The downshifting of the rather localized *d* states described here is similar to the method used to calculate the pressure-induced structural transformations of tin.[32]

As seen, SIC, GGA, and downshifting of the 3*d* states (being completely different approaches) all result in an improvement of the conventional LDA picture. The underlying physics is, to our understanding, the following: The conventional LDA approach fails to describe properly the localization of *d* states which are fully occupied in Zn. Indeed, the underestimation of their localization yields an increased *d*-*p* hybridization and thus an additional positive contribution to the pressure, which contracts the lattice. It is most probably connected with a poor description of the on-site Coulomb potential for these fully occupied states. While SIC resolves the problem in the most rigorous way, it is not surprising that the downshifting of the *d* states also works well. Both of these corrections result in an increase of *d*-state localization which reduces the *d*-*p* hybridization and in turn corrects the *d*-state contribution to the energy of chemical bonding. It is worthwhile noting that the LDA+$U$ approach (see, for example, Ref. 33) should also work well for the system considered. Since the (rather localized) 3*d* states are all below the Fermi level this approach will mainly shift these down in energy, and the LDA+$U$ will be reminiscent of the simple downshift method.[32] It was a matter of convenience for us to choose which technique to use in our investigations. We decided to use the FP-LMTO method,[26,34] which we have successfully used for simulating the effects of pressure on the lattice dynamics of high-temperature superconductors,[35–37] combined with the generalized gradient approximation. To this end we implemented the newest, to our knowledge, ''simple'' version of the GGA to the local density functional by Perdew, Burke, and Ernzerhof (PBE-GGA) (Ref. 22) within the framework of the FP-LMTO method.[26,34]

In order to test the new correction, we calculated the equilibrium volume parameters and bulk moduli for 3*d*, 4*d*, and 5*d* transition metals.[38] The PBE-GGA scheme contains an intrinsic uncertainty in a coefficient $\kappa$ [Eq. (14) in Ref. 22], which is derived from an inequality relation that gives some degree of freedom in choosing its value. Physically, $\kappa$ reflects the degree of localization of the exchange-correlation hole. We found that the originally proposed[22] value of 0.804 works well for all nonmagnetic 3*d* transition metals. However, it should be considerably decreased in order to obtain lattice parameters for 4*d* and 5*d* metals in agreement with experiment. This is in line with the suggestions from the original PBE paper[22] and obviously reflects the fact that the exchange-correlation hole gets more diffuse for heavier elements. It also stresses the need for finding universal relation between $\kappa$ and the charge density gradient, $\nabla^2 n/(2k_F)^2$. Since the value of 0.5 was found to be appropriate for 4*d* metals, we used it for hcp Cd. This stresses again that the degree of *d*-electron localization is of crucial importance for getting correct structures for Zn and Cd.

As regards other parameters in our FP-LMTO calculations, we used the triple-$\kappa$ basis set (here $\kappa=\sqrt{E}$ is an energy of Hankel and Bessel functions, not to be confused with the $\kappa$ in the PBE-GGA scheme referred to above), with the maximum angular momentum $l_{\max}\leqslant 3$ for the first, $l_{\max}\leqslant 2$ for the second, and $l_{\max}\leqslant 1$ for the third energy channel ($\kappa^2=-0.01$, $-1.0$, and $-2.3$ Ry). The basis set was formed from $3s^2 3p^6 3d^{10} 4s^1, 4p^0, 4f^0$ for Zn and $4s^2 4p^6 4d^{10} 5s^1$, $5p^0, 4f^0$ orbitals for Cd with ''semicore'' Zn $3s^2 3p^6$ and Cd $4s^2 4p^6$ orbitals treated as localized orbitals[34] in the spirit of Singh.[39] The calculations were performed in a spin-restricted scalar-relativistic mode. No spin-orbit coupling was taken into account. We used muffin-tin radii of 2.45 a.u. for Zn and 2.75 a.u. for Cd at their experimental lattice parameters, respectively, which were then scaled in the pressure simulation according to the unit cell volume changes. The charge density was calculated in the muffin-tin spheres for angular momentum components up to $l_{\max}=7$. The same $l$ cutoff was used when interpolating the charge density in the interstitial region over Hankel functions with energies of $-1$ and $-3$ Ry. We found the results to depend critically on the number of sampling $k$ points. Only starting from 12 000 $k$ points in the full Brillouin zone can one obtain reliable results for both the lattice parameters and the electric-field gradient tensor. This fact was pointed out also in earlier studies.[8,13] To ensure

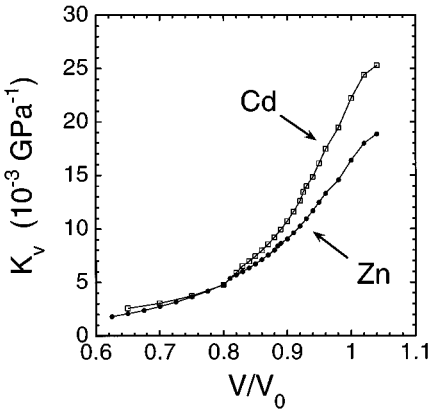


FIG. 4. Dependence of the volume compressibility ($K_v$) on pressure for hcp Zn and Cd.

reliability of our results we used 24 000 $k$ points in the full Brillouin zone (BZ).

In order to find the equilibrium lattice parameters, we calculated the total energy of hcp Zn and Cd for a wide range of $c/a$ values for the unit cell volumes starting from $V/V_0=1.04$ ($V_0$ is the experimental unit cell volume) to 0.6 in steps of 0.01 and reducing them to 0.005 in a volume range where the $c/a$ anomaly takes place. We have to note also that the use of atomic forces in conjunction with the usual minimization algorithms to find equilibrium $c/a$ for a particular unit cell volume was impossible, since the total-energy dependence on $c/a$ shows a double well structure in the region of the anomaly. Finally, the Brillouin zone integrations were performed using a weighted sum integration with a smearing parameter of 2 mRy.

## III. RESULTS AND DISCUSSION

### A. Equation of state and bulk moduli for hcp Zn and Cd

In order to check the quality of our simulations, we calculated the equation of state, $V(P)$, the volume compressibility, and bulk modulus as a function of hydrostatic pressure for Zn and Cd. Figure 2 shows the total-energy dependence on volume ($V/V_0$) for Zn and Cd for the whole range of volumes considered and the insets present $E(V/V_0)$ dependencies in a region around their minima. Each point

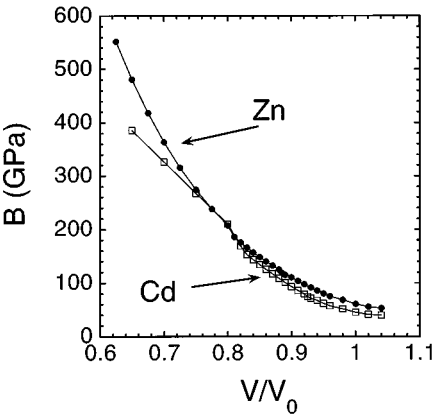


FIG. 5. Dependence of the bulk modulus ($B$) on pressure for hcp Zn and Cd.

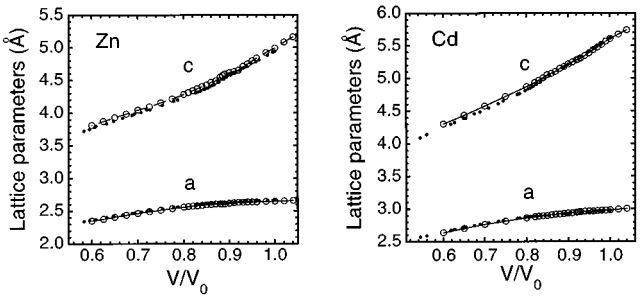


FIG. 6. The calculated (open circles) and experimental (dots) (Refs. 12, 27, and 40) lattice parameters of hcp Zn and Cd as a function of relative volume.

represents a result of a ($c/a$) total-energy optimization for a particular volume. From this we then calculated the equation of state, $V(P)$, for both metals (cf. Fig. 3). The pressure was estimated as a total-energy derivative [$P=-\partial E(V)/\partial V$], and was calculated analytically from a sixth-order polynomial fit to the total-energy results. A comparision with the experimental results by Takemura for Zn[12,27] and Cd (Ref. 40) shows excellent agreement of the theory for low pressures, while for higher pressures one can see an increasing deviation of our theoretical curves from experiment. It would appear that a similar overestimation of the pressures at small volumes was already seen (in Fig. 1) for all computational techniques used to obtain the correct equilibrium volume for Zn in Sec. II. Although, the $3d$-downshift correction, if used, should in fact be reduced as the bandwidth is increased due to the compression, and at very small volumes this calculation would approach the LDA result. As mentioned earlier, the experiments also seem to agree with this. The SIC may also exhibit such behavior. It remains to be investigated whether a similar reduction of localization may be reflected in a reduction of the parameter $\kappa$ in the PBE-GGA that is sufficient to bring the high pressure results closer to experiment. The theoretical pressure dependence of the volume for Cd is also in good agreement with (i) the experimental compression curve (cf. Fig. 3 of Ref. 41) derived by using the equation of state[42] and (ii) recent measurements.[40] The theoretical equilibrium volumes corresponding to zero pressure are $V/V_0=1.005$ for Zn and 0.992 for Cd.

Figure 4 shows the pressure dependence of the volume compressibility [$K_V=-(1/V)(\partial V(P)/\partial P)$] of Zn and Cd. As seen, for a wide range of volumes (from $V/V_0=1$ to 0.8) Cd is more compressible than Zn while at high pressures

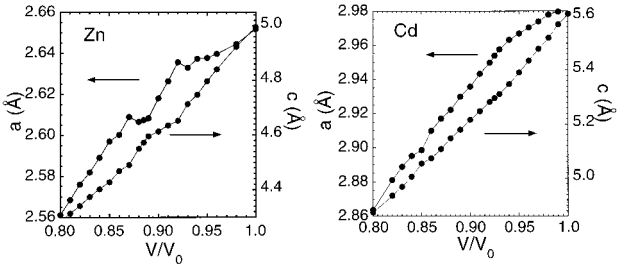


FIG. 7. The calculated lattice parameters of hcp Zn and Cd in the low pressure region.

TABLE I. Theoretical ($T=0$ K) and room-temperature experimental data for bulk modulus ($B$, GPa), volume compressibility ($K_V$), and $a$- and $c$-axis compressibilities ($K_a$ and $K_c$) in units of GPa$^{-1}$.

| | $B^{\text{theor.}}$ | $B^{\text{exper.}}$ | $K_V^{\text{theor.}}$ | $K_V^{\text{exper.}}$ | $K_a^{\text{theor.}}$ | $K_a^{\text{exper.}}$ | $K_c^{\text{theor.}}$ | $K_c^{\text{exper.}}$ |
|---|---|---|---|---|---|---|---|---|
| Zn | 59.5 | 56.5 (Ref. 43) | 16.8 | 17.7 (Ref. 43) | 1.5 | 1.9 (Ref. 43) | 13.8 | 14.0 (Ref. 43) |
| | | 59.8 (Ref. 44) | | 16.7 (Ref. 44) | | 1.5 (Ref. 3) | | 13.3 (Ref. 3) |
| | | 58.0 (Ref. 12) | | | | 1.6 (Ref. 45) | | 13.8 (Ref. 45) |
| Cd | 45.9 | 45.7 (Ref. 43) | 21.8 | 21.9 (Ref. 43) | 2.4 | 2.5 (Ref. 43) | 17.0 | 17.0 (Ref. 43) |
| | | 47.6 (Ref. 41) | | 21.0 (Ref. 41) | | 2.3 (Ref. 41) | | 16.5 (Ref. 41) |
| | | 46.7 (Ref. 44) | | 21.4 (Ref. 44) | | | | |

(starting from $V/V_0=0.8$) their respective compressibilities are practically equal. Figure 5 displays the pressure dependence of the bulk moduli ($B=K_V^{-1}$) of these metals. The bulk moduli for Zn and Cd at zero pressure were found to be in excellent agreement with experimentally measured ones (cf. Table I). This kind of agreement between theoretical and experimental bulk moduli is unusual since it is widely accepted that the LDA error in their estimation is usually around 15–30 %.

### B. Lattice parameters, $c/a$ ratio, and axis compressibilities

Figure 6 presents the calculated dependence of the $a$ and $c$ lattice parameters on the unit cell volume for Zn and Cd together with experimental results[12,40] for the whole range of unit cell volumes considered, while Fig. 7 shows this dependence in the low pressure region. The calculated pressure dependence of the lattice parameters is found to be in good agreement with experiment. These calculations predict anomalous volume dependences of $c$ as well as $a$ in both metals. The anomaly is somewhat more pronounced in $a$ than in $c$. This might explain why only the $a$-axis anomaly was detected experimentally (cf. Fig. 4 in Ref. 12). The calculated and experimental pressure dependence of $c/a$ for Zn and Cd is plotted in Fig. 8. As seen, the calculations consistently overestimate $c/a$ at higher pressures for both Zn and Cd, although the maximum discrepancy does not exceed 2%. In the low pressure region, the theoretical $c/a$ values deviate from experiment by less than 1%.

The theoretical pressure dependence of $c/a$ clearly shows anomalies for both Zn and Cd. The volume at which the anomaly takes place in Zn is $V/V_0=0.89$ which corresponds to a theoretical pressure of $P=9$ GPa and for Cd one can see two kinks on the theoretical $c/a$ curve: the first at $V/V_0=0.92$ and a second at 0.85. Actually, one can regard this as a single, rather broad anomaly that spans the region of $V/V_0$ from 0.92 to 0.85, especially if as will be discussed later we take into account the uncertainty in the $c/a$ determination. The consistent overestimation of $c/a$ at higher pressures may appear due to several reasons: (i) From the experimental side, there can be a nonzero pressure gradient at high pressures which may contribute to the deviation from hydrostatic conditions. In this case, it is very likely that the $c$ axis would be compressed at a faster rate and thus contribute to the decrease of the $c/a$ ratio, since we show later in the paper that the compressibility of the $c$ axis is indeed much higher than that for the $a$ axis. (ii) From the theoretical side we may guess that the GGA correction does not scale well with volume. This possibility needs to be investigated in the future. We have examined the effect of including spin-orbit coupling: over a wide volume and $c/a$ range the total-energy results are not affected.

In order to demonstrate the highly anisotropic lattice properties of hcp Zn and Cd, we calculated the $c$- and $a$-axis compressibilities. Generally, the compressibility along a given axis, $\alpha$, is defined as $K_\alpha=-(1/\alpha)(\partial\alpha(P)/\partial P)$. Its dependence on relative volume was calculated analytically from a fit to $a(P)$ and $c(P)$ in the low and high pressure regions (above and below the anomaly region) and by using numerical differentiation of $a(P)$ and $c(P)$ in the anomaly region for both Zn and Cd (cf. Fig. 9). In the absence of external pressure, $K_c$ is several times greater than $K_a$, which clearly displays the highly anisotropic lattice properties of these metals. The axis compressibilities decrease monotonically when pressure is applied, with $K_c$ decreasing much faster than $K_a$. Finally, at pressures corresponding $V/V_0=0.7$ they become practically equal. For both metals, both $K_a$ and $K_c$ show nonmonotonic behavior [the pressure derivative of $a(P)$ and $c(P)$ diverges or changes rapidly] around the volume at which the $c/a$ anomaly takes place (cf. Fig. 8). A comparison of the axis compressibilities ($K_a$ and

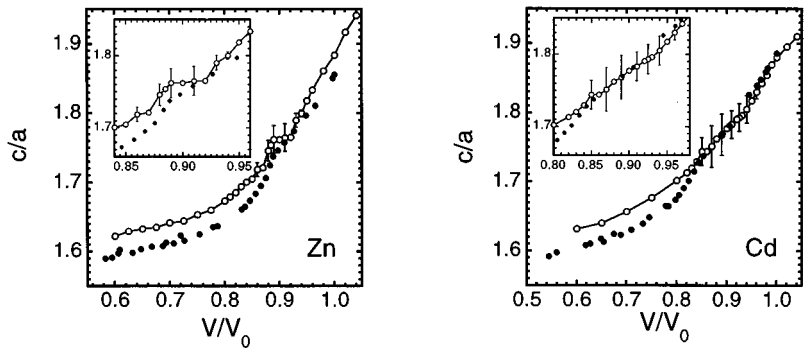


FIG. 8. The calculated (open circles) and experimental (dots) (Refs. 12, 27, and 40) change of $c/a$ for hcp Zn and Cd as a function of relative volume. Error bars indicate the $c/a$ region where the total energy is essentially flat (see discussion in the text). The insets show the $c/a$ dependence around the anomaly region.

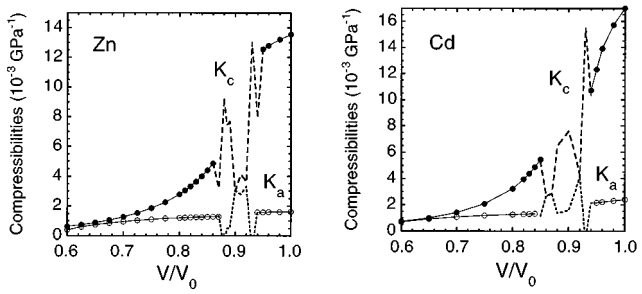


FIG. 9. The calculated axis compressibilities ($K_a$ and $K_c$) of hcp Zn and Cd as a function of relative volume.

$K_c$) for Zn and Cd at zero pressure with experiment is given in Table I and shows good agreement.

Such a peculiar dependence of the lattice parameters on pressure (in a certain pressure region) arises from a very unusual total-energy dependence on $c/a$ in a $V/V_0$ interval around the anomaly. Figure 10 shows the $E(c/a)$ curve (filled circles) for Zn at different $V/V_0$ (the results for Cd look similar). The total-energy curve is parabolic in the volume region from $V/V_0=1$ to 0.92 (not shown in Fig. 10), then becomes distorted at $V/V_0=0.91$ but still retains a single, well pronounced minimum. For smaller volumes

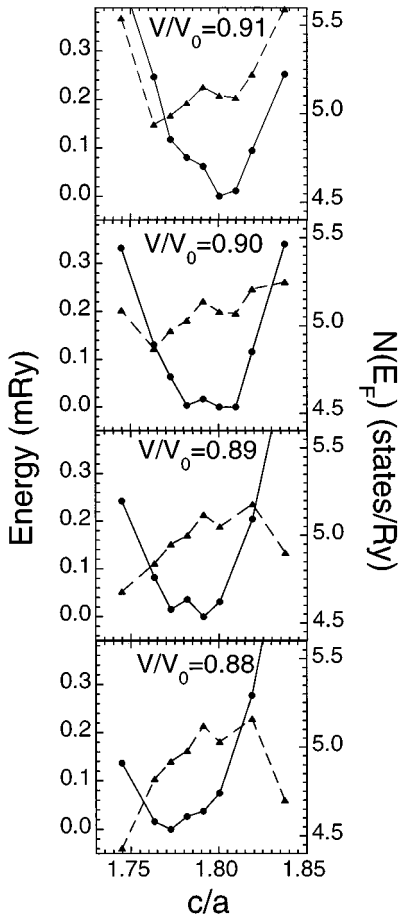


FIG. 10. Total energy (circles) and the total density of states at $E_F$ (triangles) as functions of $c/a$ for hcp Zn at different volumes around the anomaly region.

($V/V_0=0.90$ and 0.89), the distortion propagates further producing a double-well shape of $E(c/a)$ around its minimum. The energy barrier is extremely small (around 0.03 mRy or 4–5 K) and an accurate determination of its height is beyond the precision of the method. At finite (even rather low) temperatures, the total energy in this $c/a$ region appears essentially flat. (But the appearance of the double-well structure, which was also found earlier,[20,21] indicates that at $T=0$ the structural change at $c/a\approx 1.73$ is a first-order transition.) The range of $c/a$ values for which the $E(c/a)$ curve is essentially flat is quite large, about 0.03. This makes it difficult to find an exact minimum for $E(c/a)$. Also, this is the reason why we could not use the calculation of atomic forces for the $c/a$ optimization.

A similar shape of the total energy versus $c/a$ was also found for Cd for relative volumes in the range from 0.92 to 0.85. In this anomalous regime we took the equilibrium $c/a$ to be at the center of the flat (or double-well) region, and we indicate the possible range of $c/a$ values by error bars in Fig. 8. In an attempt to understand the reason for such a specific shape of the total energy, we calculated the energy band structure for Zn (at $V/V_0=0.90$) for different $c/a$ values along all high-symmetry directions in the BZ, but found no remarkable changes in band positions that could be responsible for the effect. However, the total density of states at the Fermi level, $N(E_F)$, as a function of $c/a$ presented in Fig. 10 (filled triangles) definitely shows a local enhancement of $N(E_F)$ coinciding with the center of the double well. This local enhancement is very small (about 0.05–0.1 Ry$^{-1}$) and can hardly be attributed to any kind of electronic topological transition. The most probable reason for such a peculiar total-energy dependence is a delicate balance in the in-plane and interplanar chemical bonding in the hcp structure. A loss in total energy caused by an in-plane lattice expansion is exactly compensated by a gain in the energy due to the interplanar distance contraction. We speculate that the dramatic phonon softening found in Ref. 13 might be directly related to the specific (flat or double-well) shape of the total-energy curve in the ''anomaly region.'' Moreover, a flat potential can also indicate the possibility of a pressure-induced phase disorder in the system (coexistence of hcp Zn or Cd phases with different $c/a$) which in turn could drastically affect the physical properties of these metals.

In fact, an anomalous behavior of the resistivity in Zn and Cd under pressure was detected by Lynch[15] exactly at pressures corresponding to the lattice anomalies in both metals. It was found that the resistivity displays a local maximum in this pressure region which can be understood from a drastic phonon softening in the anomaly region. The phonon softening increases the probability of electron scattering giving rise to the resistivity. Clearly, an *ab initio* investigation of phonon properties under pressure is needed.

### C. Electric-field gradient

The dependence of the electric-field gradient on hydrostatic pressure in hcp Zn was first measured by Potzel *et al.*[13] and calculated[14] using the FLAPW method.[25] While the experimental data show a change in the slope of the pressure dependence of the main component, $V_{zz}$, of the EFG tensor at the pressure corresponding to the $c/a$ anomaly, the calcu-

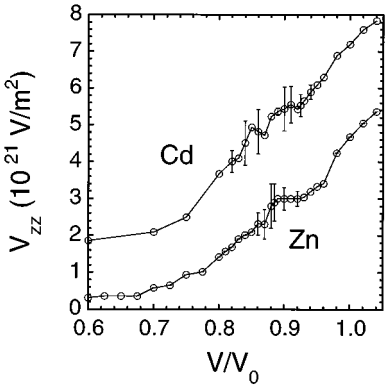


FIG. 11. Theoretical volume dependence of the main component $V_{zz}$ of the electric-field gradient tensor for hcp Zn and Cd. Error bars indicate the uncertanties induced by a flat total-energy region for $c/a$, as discussed in the text.

lations were not able to detect any such anomaly. On the other hand, if an anomaly in $c/a$ does exist, it is very likely to induce a corresponding anomaly in $V_{zz}$. This simply follows from the results of the same authors,[14] which show that the main contribution to the decrease of the EFG in hcp Zn under external pressure is essentially determined by the decrease of $c/a$. In order to resolve this controversy, we calculated the pressure dependence of EFG using our optimized $c/a$ values for all volumes considered and for both metals.

The main component was found always to be two times larger than the $V_{xx}$ and $V_{yy}$ components, which in turn are equal due to the symmetry properties of the hcp lattice. Figure 11 shows the pressure dependence of $V_{zz}$ in Zn and Cd. As seen, the shape of the volume dependence $V_{zz}$ is very similar to the $c/a$ vs $V/V_0$ curve (cf. Fig. 8) for both metals. The anomaly in $V_{zz}$ exists at the same $V/V_0$ value as for $c/a$. This contradicts the conclusions of Ref. 14 that hydrostatic pressure has little or no effect on the EFG tensor in Zn. The experimental values of $V_{zz}$ for Zn are lower than the calculated ones, but the overall volume dependence of $V_{zz}$ agrees well with experiment and exhibits the slope decrease for higher pressures. Again, we note that the flatness of $E(c/a)$ in the anomaly region yields a region of $c/a$ values with constant energy and in turn induces a corresponding uncertainty region in the EFG tensor which is marked in Fig. 11 by error bars.

### D. Band structure and density of states

Finally, we discuss the effects of pressure on the band structure and its impact on such an important characteristic of metals as the total density of states at the Fermi level. Figure 12 shows the band structure of Zn for six different unit cell volumes and demonstrates that the band structure of hcp Zn changes considerably with pressure (the band structure of Cd behaves similarly). First, note that for higher pressures the position of the Zn 3*d* states (i.e., the dense group of bands around $-8$ eV below $E_F$) shifts consistently down in energy relatively to $E_F$ and the bands become more dispersed. Another interesting feature of the Zn band-structure transformation with pressure is that starting from $V/V_0=0.75$ a band gap opens in the $ALH$ plane in the BZ.

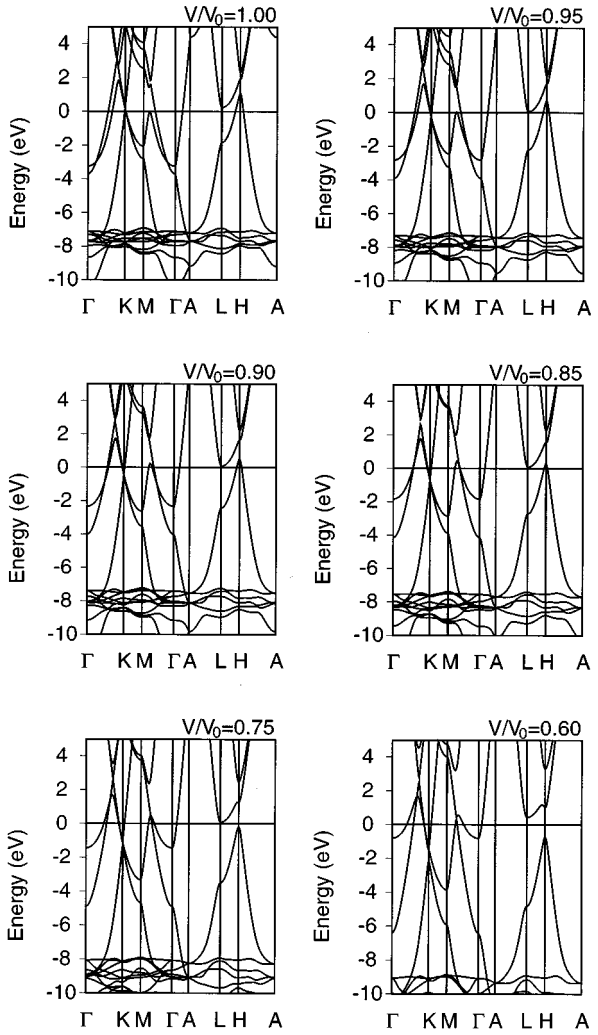


FIG. 12. FP-LMTO band structure along some high-symmetry directions of hcp Zn for different relative volumes.

We paid special attention to the position of the band located at the $L$ point in the BZ since it was thought[13,14] to be responsible for all kinds of anomalies observed in hcp Zn. Indeed, if this band were to cross $E_F$, the topology of the Fermi surface changes since the states at point $L$ become occupied. In turn, this ETT would then cause the destruction of the giant Kohn anomaly which might in turn lead to sudden changes in the phonon system. However, as seen from Fig. 12, the band at the $L$ point never falls below $E_F$ even for the highest pressures considered. Actually, we found that its energy position depends crucially on the $c/a$ parameter: for smaller $c/a$ values the band does shift below $E_F$, but it becomes increasingly energetically unfavorable (i.e., the total energy increases rapidly once this band becomes occupied). The fact that we found the $c/a$ anomaly in Zn and Cd, despite the absence of any such ETT acompanied by a destruction of the giant Kohn anomaly, indicates that this specific ETT is not responsible for the appearance of the anomaly. Thus, our results do not confirm the view expressed in Refs. 13,14 on the nature of the lattice anomalies in hcp Zn.

Unfortunately, we were unable to pinpoint a specific band-structure change that might be responsible for the

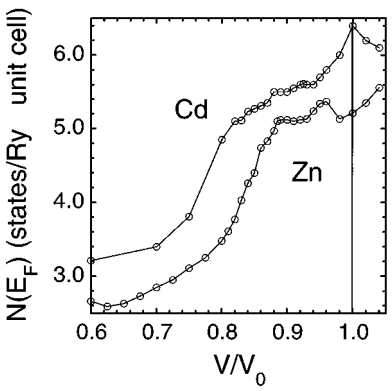


FIG. 13. Total density of states at $E_F$ for hcp Zn and Cd as a function of relative volume.

anomalous lattice behavior of hcp Zn and Cd under pressure. It turns out to be instructive to analyze the behavior of the total density of states at the Fermi level, $N(E_F)$, under pressure, which provides a more average view on electronic structure transformations with pressure. Figure 13 presents calculated values of $N(E_F)$ as a function of the unit cell volume for Zn and Cd. Normally, for an almost-free electron metal one would expect a monotonic decrease of $N(E_F)$ at reduced volumes due to increased band dispersion. However, $N(E_F)$ for both Zn and Cd displays a local enhancement exactly around the volume region where the anomaly in $c/a$ and EFG takes place. Such local $N(E_F)$ enhancement is most probably the source of the anomalies studied in this paper. It might be connected with a complicated Fermi surface transformation and related to the interplay of in-plane and interplanar chemical interactions under pressure. Note also that the nonmonotonic behavior of $N(E_F)$ is more pronounced in Zn than in Cd, which might explain the fact that the $c/a$ anomaly in Zn is stronger than in Cd—as discussed earlier.

## IV. CONCLUSIONS

Our first-principles full-potential LMTO investigations of the electronic structure, lattice parameters, and EFG tensor for hcp Zn and Cd under hydrostatic pressure are found to reproduce correctly the experimentally found anomaly in $c/a$ at $V/V_0 = 0.89$ in hcp Zn. We also predict a similar anomaly in hcp Cd for $V/V_0 = 0.92$ which is less clearly pronounced and might be more difficult to detect experimentally. The EFG tensor also exhibits an anomalous behavior at the same $V/V_0$ values where the $c/a$ anomaly takes place in both metals. Our analysis does not support the idea that an ETT that causes the destruction of the giant Kohn anomaly is primarily responsible for the lattice anomalies in hcp Zn and Cd.

From the methodological point of view we showed that the recently developed generalized gradient approximation to the local density functional by Perdew, Burke, and Ernzerhof yields accurate equilibrium volumes and bulk moduli for hcp Zn and Cd, where the pure LDA fails. Other correction methods that reduce the $d$-$p$ hybridization by downshifting the $d$ states relative to their LDA energies also work well in this respect.

## ACKNOWLEDGMENTS

We are grateful to K. Takemura for communicating his experimental data prior to publication and for very useful discussions, and thank A. Shick, W. Mannstadt, and A. Liechtenstein for their criticisms and fruitful discussions. Work at Northwestern University was supported by the National Science Foundation (DMR 91-20000) through the Science and Technology Center for Superconductivity, and by a grant of computer time at the NCSA, University of Illinois Urbana–Champaign and at the Pittsburgh Supercomputing Center. Work in Denmark and Argentina was supported by the Danish Natural Science Research Council (Grant No. 11-9685-1) and the Commission of the European Communities, Contract No. CI1*-CT92-0086.

*On leave from the Institute of Solid State Chemistry, Russian Academy of Sciences, Yekaterinburg, Russia. Electronic address: d-novikov@nwu.edu

[1] W. Potzel, U. Närger, T. Obenhuber, J. Zänkert, W. Adlassing, and G. M. Kalvius, Phys. Lett. **98A**, 295 (1983).
[2] G. Borgonovi, G. Caglioti, and J. Antal, Phys. Rev. **132**, 683 (1963).
[3] G. A. Alers and J. R. Neighbours, J. Phys. Chem. Solids **7**, 58 (1958).
[4] L. Almqvist and R. Stedman, J. Phys. F **1**, 785 (1971).
[5] W. Potzel, W. Adlassnig, J. Moser, C. Schäfer, M. Steiner, and G. M. Kalvius, Phys. Rev. B **39**, 8236 (1989).
[6] A. S. Ivanov, N. L. Mitrofanov, V. V. Pushkarev, A. Y. Rumyantsev, and N. A. Chernoplekov, Fiz. Tverd. Tela **28**, 767 (1986) [Sov. Phys. Solid State **28**, 427 (1986)].
[7] T. P. Das and P. C. Schmidt, Z. Naturforsch. Teil A **41**, 47 (1986).
[8] P. Blaha, K. Schwarz, and P. H. Dederichs, Phys. Rev. B **37**, 2792 (1988).
[9] P. Blaha, Hyperfine Interact. **60**, 773 (1990).
[10] S. Meenakshi, V. Vijayakumar, B. K. Godwal, and S. K. Sikka, Phys. Rev. B **46**, 14 359 (1992).
[11] D. Singh and D. A. Papaconstantopoulos, Phys. Rev. B **42**, 8885 (1990).
[12] K. Takemura, Phys. Rev. Lett. **75**, 1807 (1995).
[13] W. Potzel, M. Steiner, H. Karzel, W. Schiessl, M. Köfferlein, G. M. Kalvius, and P. Blaha, Phys. Rev. Lett. **74**, 1139 (1995).
[14] M. Steiner, W. Potzel, H. Karzel, W. Schiessl, M. Köfferlein, G. M. Kalvius, and P. Blaha, J. Phys: Condens. Matter **8**, 3581 (1996).
[15] R. W. Lynch and H. G. Drickamer, J. Phys. Chem. Solids **26**, 63 (1965).
[16] O. Schlute, A. Nikolaenko, and W. B. Holzapfel, High Press. Res. **6**, 169 (1991).
[17] E. Bodenstedt, B. Perscheid, and S. Nagel, Z. Phys. B **63**, 9 (1986).
[18] Y. Kagan and V. V. Pushkarev, Zh. Éksp. Teor. Fiz. **84**, 1494 (1982) [Sov. Phys. JETP **57**, 870 (1983)].
[19] A. A. Chernyshov, V. V. Pushkarev, A. Y. Rumyantsev, D. B., and R. Pynn, J. Phys. F **9**, 1983 (1979).
[20] N. E. Christensen (unpublished).
[21] T. Brudevoll and N. E. Christensen, Bull. Am. Phys. Soc. **41**, 717 (1996).
[22] J. Perdew, K. Burke, and M. Ernzerhof, Phys. Rev. Lett. **77**, 3865 (1996).

[23] O. K. Andersen, Phys. Rev. **12**, 3060 (1975).
[24] D. D. Koelling and G. O. Arbman, J. Phys. F **5**, 2041 (1975).
[25] E. Wimmer, H. Krakauer, M. Weinert, and A. J. Freeman, Phys. Rev. B **24**, 864 (1981), and references therein.
[26] M. Methfessel, Phys. Rev. B **38**, 1537 (1988).
[27] K. Takemura (private communication).
[28] Full-potential LMTO code developed by J. Wills, Los Alamos National Laboratory, New Mexico.
[29] A. Svane and O. Gunnarsson, Phys. Rev. Lett. **65**, 1148 (1990).
[30] A. Svane, Phys. Rev. B **53**, 4275 (1996).
[31] J. P. Perdew, J. Chevary, S. Vosko, K. Jackson, M. Pederson, D. Singh, and C. Fiolhais, Phys. Rev. B **46**, 6671 (1992).
[32] N. E. Christensen and M. Methfessel, Phys. Rev. B **48**, 5797 (1993).
[33] A. I. Liechtenstein, V. I. Anisimov, and J. Zaanen, Phys. Rev. B **52**, R5467 (1995).
[34] M. van Schilfgaarde (unpublished).
[35] D. L. Novikov and A. J. Freeman, Physica C **219**, 246 (1993).
[36] D. L. Novikov and A. J. Freeman, Physica C **222**, 38 (1994).
[37] D. L. Novikov, M. I. Katsnelson, J. Yu, A.V. Postnikov, and A. J. Freeman, Phys. Rev. B **54**, 1313 (1996).
[38] D. L. Novikov and A. J. Freeman (unpublished).
[39] D. Singh, Phys. Rev. B **43**, 6388 (1991).
[40] K. Takemura, Phys. Rev. B (to be published).
[41] G. A. Saunders and Y. K. Yogurtcu, J. Phys. Chem. Solids **47**, 421 (1986).
[42] F. D. Murnaghan, Proc. Natl. Acad. Sci. USA **30**, 244 (1944).
[43] Present authors values based on data of Ref. 40.
[44] C. Kittel, *Introduction to Solid State Physics* (Wiley, New York, 1996).
[45] P. W. Bridgman, Phys. Rev. **47**, 393 (1945).